

## CHAPTER 2

### Hydrophobic Protection of Heme in Zn-cytochrome *c*

#### *Acknowledgment*

Experiments were done in collaboration with Dr. Judy E. Kim. This chapter is adapted in part from Kim, J.E.; Pribisko, M.A.; Gray, H.B.; Winkler, J.R. Zinc-porphyrin Solvation in Folded and Unfolded States of Zn-cytochrome *c*. *Inorg. Chem.* **2004**, *43*, 7953-7960. Please note that some figures were created with help from Dr. Brian S. Leigh.

## 2.1 INTRODUCTION

Although proteins have a very intimate and rich relationship with water, our understanding of this interaction is limited and difficult to extract. In particular, little is known of the solvent-mediated interactions that are essential during the process of protein folding. Water expulsion and inclusion are crucial for native structures,<sup>1</sup> protein-protein recognition,<sup>2</sup> and folding pathways.<sup>3-6</sup> Both folded and unfolded protein structures are associated with solvent molecules,<sup>7,8</sup> and chemical denaturant activity is attributed to changes in water hydrogen bonding networks as well as direct solvation of peptide bonds and hydrophobic residues.<sup>9,10</sup> Molecular dynamics simulations<sup>3,4</sup> suggest that rapidly-formed, collapsed structures trap a significant number of water molecules that may expedite hydrogen bond formation along the backbone chain as well as facilitate structural transitions. NMR studies have shown that buried water molecules have longer residence times than water located near the surface of the protein.<sup>6,7</sup> In addition, computational studies indicate that the expulsion of water molecules from the core of the protein might be one of the final steps in protein folding.<sup>8</sup> All of the pieces of information sum to underscore the importance of water in protein folding, but provide little specific data on the interplay of water while a protein is folding. While these and other computational studies have aimed to elucidate the role of water in protein structure and folding, very few experiments have probed the dynamics of solvation during a folding reaction.

### 2.1.2 Measures of Zn-porphyrin Solvation

X-ray crystal structures reveal water molecules found in close proximity to the heme in horse heart cytochrome *c*, leading one to believe water is important structurally

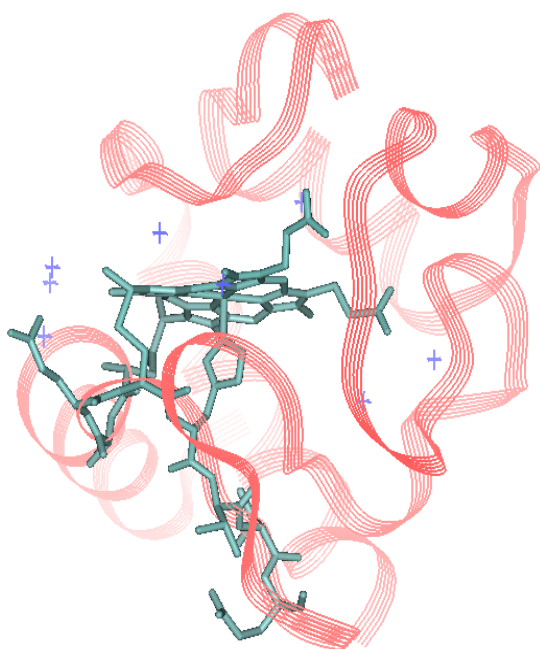


**Figure 2.1.** The structure of MP8, which consists of the heme group plus residues 14-21, is shown in green in horse heart cytochrome *c* (PDB file 1HRC).<sup>42</sup> Water molecules within 5 Å of the heme are indicated by blue symbols.

and/or functionally.<sup>4,5</sup> As a model system for probing the interactions of protein and solvent during the folding reaction, we use cytochrome *c* modified through zinc-substitution of the porphyrin cofactor. Zn-cyt *c* is structurally similar to the native protein (Fe-cyt *c*), which has been studied in great detail.<sup>11,12,13</sup> NMR and crystal structures of Zn-cyt *c*, Fe(II)-cyt *c*, and Fe(III)-cyt *c* reveal only minor differences

in backbone positions, identical His18 and Met80 axial ligands, and unchanged porphyrin environments upon Zn(II)

substitution.<sup>14,15</sup> The stability of folded Zn-cyt *c* ( $\Delta G_f^\circ = -35$  kJ/mol) is comparable to that of the Fe(III) form ( $\Delta G_f^\circ = -40$  kJ/mol); however both are less stable than Fe(II)-cyt *c* ( $\Delta G_f^\circ = -74$  kJ/mol).<sup>16,17</sup> The structural and thermodynamic similarities to native Fe-cyt *c*, the existence of a long-lived, solvent-sensitive triplet state, and the lack of axial ligand traps make Zn-cyt *c* an ideal system for investigations of the role of hydration in folding.

Furthermore, this system was chosen because its optical properties are both sensitive to the solvent environment and readily measurable through time-resolved spectroscopy. Upon photon absorption, rapid and efficient (quantum yield  $\sim 0.9$ )<sup>18</sup> intersystem crossing creates a long-lived porphyrin triplet state whose deactivation depends strongly on outer sphere solvation. Strong coupling to vibrational modes of the

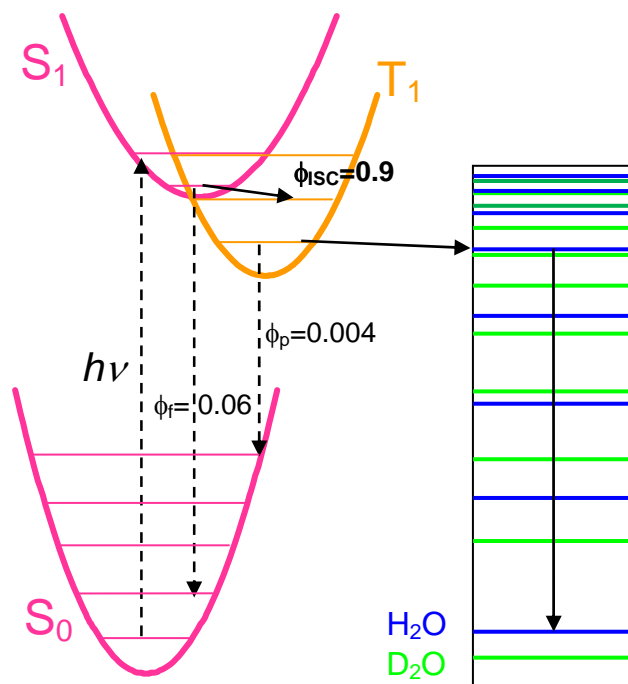


**Figure 2.2.** Deactivation of Zn-porphyrin triplet excited states through vibronic coupling to a high-frequency water stretch mode. Dashed lines are optical transitions and solid lines are radiationless events. Fluorescence and phosphorescence quantum yields are noted, as well as that of the singlet (S<sub>1</sub>) to triplet (T<sub>1</sub>) intersystem crossing.

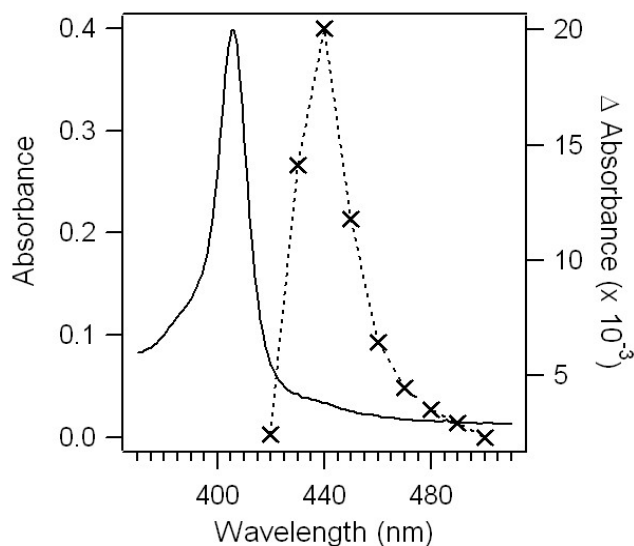


**Figure 2.3.** Ground-state (solid, left axis) and triplet transient (---X---, right axis) absorption spectra of  $\sim 2 \mu\text{M}$  ZnAcMP8 in 20 mM phosphate + 0.1% TFA solution.

porphyrin and the first solvent shell efficiently converts the  $>13,000\text{ cm}^{-1}$  of electronic energy to vibrational energy, enhancing the nonradiative triplet decay rate (Figure 2.2).<sup>19,20,21</sup> Since the triplet excited state is very reducing ( $E^0 = -0.8\text{ V vs. NHE}$ ), an external oxidant such as  $\text{Ru}(\text{NH}_3)_6^{3+}$  ( $E^0 = 0.06\text{ V vs. NHE}$ ) is easily reduced and provides an alternative path for triplet state deactivation and another measure for heme salvation.<sup>22</sup>

As outlined in Figure 2.4, quenching of the triplet state proceeds with high driving force ( $-\Delta G^0 = 0.9\text{ eV}$ ), creating a Zn-porphyrin cation radical and  $\text{Ru}(\text{NH}_3)_6^{2+}$  (Reaction B) that subsequently react to reform ground-state Zn-porphyrin and

$\text{Ru}(\text{NH}_3)_6^{3+}$  (Reaction C).<sup>23</sup>

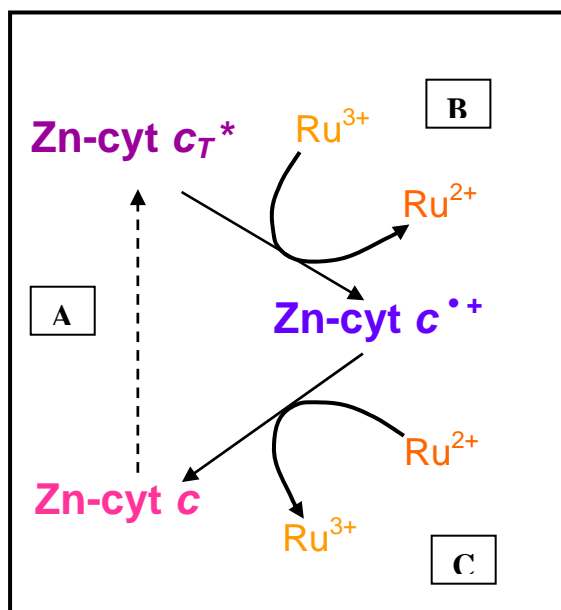


**Figure 2.4.** Electron transfer to external quencher. Zn-cyt c triplet excited state is denoted Zn-cyt  $c_T^*$  and radical cation state is Zn-cyt  $c^{\bullet+}$ .

The degree to which there is an isotope effect or efficient triplet decay in the presence of redox quenchers directly reflects the extent of hydration and solvent accessibility of the Zn-porphyrin, and hence each of these properties can report on the solvation of various conformational

states of cytochrome *c*.

Zinc-substituted N-acetyl-microperoxidase-8, ZnAcMP8, was employed to distinguish the effects of solvent coupling from intramolecular interactions on Zn-cyt *c* triplet lifetimes. MP8 is a heme octapeptide derived from enzymatic cleavage of cyt *c*

(Figure 2.1); the heme + loop region 14-18 comprises an active site whose structure is virtually the same as that in the holoprotein, including axial ligation by His18.<sup>24</sup> Because the tryptic fragment is fully exposed to the aqueous environment, it is reasonable to assume that triplet state decay rates in this case will be dominated by solvent effects. Our combined studies of Zn-cyt *c* and ZnAcMP8 shed light on the immediate solvent environment of the cofactor in equilibrium folded and unfolded states.

## **2.3 RESULTS AND DISCUSSION**

### **2.3.2 Transient Absorption Decays in Protonated and Deuterated Solvent**

Decay kinetics of the ZnAcMP8 and Zn-cyt *c* triplet states in protonated and deuterated phosphate buffers, GdmCl, and urea are shown in Figure 2.6. Triplet decays in phosphate buffer can be described by monoexponential kinetics, while decays in urea and GdmCl exhibit biphasic behavior, with major (>80%) and minor (<20%) components similar to those described previously.<sup>25</sup> The major components of the decay rates are set out in Table 2.1. The triplet state of ZnAcMP8 decays faster than those of both folded and unfolded Zn-cyt *c*, consistent with maximum solvent exposure of the cofactor in the tryptic fragment. Comparison of ZnAcMP8 photophysics in the two denaturants reveals longer lifetimes in urea relative to GdmCl. Since the vibrational spectra of the two denaturants are similar in the high frequency region, the difference in decay rates may reflect the role of ionic strength in triplet deactivation for the fully exposed Zn-porphyrin. The triplet lifetimes of folded and unfolded Zn-cyt *c* are substantially longer than that of

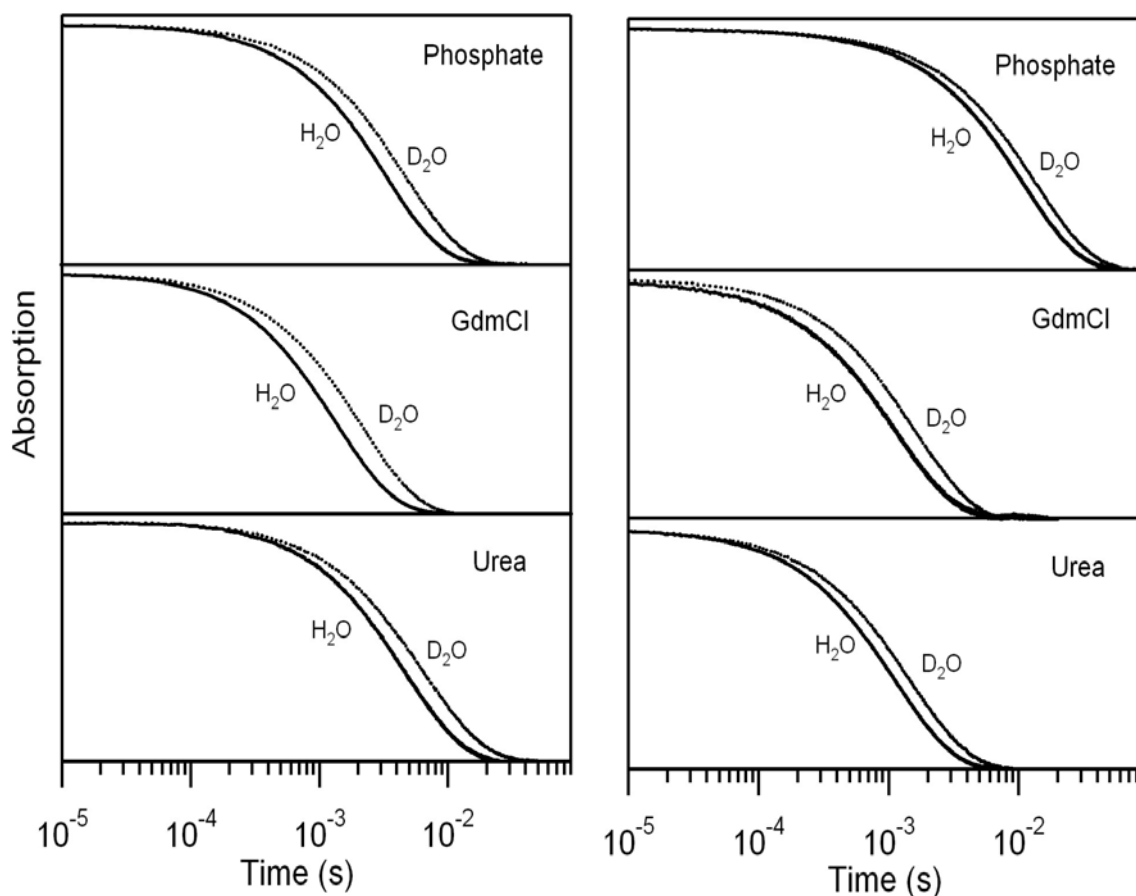


**Figure 2.5.** Transient absorption decay kinetics of triplet ZnAcMP8 (left) and Zn-cyt *c* (right) in protonated and deuterated solutions. Buffers were 20 mM phosphate (top) with ~5 M GdmCl (middle) or ~9 M urea (bottom). For ZnAcMP8, 0.1% TFA was added to the buffer; for Zn-cyt *c*, solutions were pH = pD = 7.4.

|                                     | $k_{\text{H}_2\text{O}}$ ( $\text{s}^{-1}$ ) | $k_{\text{D}_2\text{O}}$ ( $\text{s}^{-1}$ ) | $k_{\text{H}_2\text{O}}/k_{\text{D}_2\text{O}}$ |
|-------------------------------------|--|--|---|
| <b>ZnAcMP8 in phosphate</b>         | 3030   | 1990   | 1.5   |
| guanidine                           | 6980   | 4955   | 1.4   |
| <b>Zn-cyt <i>c</i> in phosphate</b> | 105  | 90   | 1.2   |
| guanidine                           | 810  | 600  | 1.4   |

**Table 2.1.** Rate constants and isotope effects for ZnAcMP8 and Zn-cyt *c* triplet states. Errors for rate constants are  $\pm 15\%$ .

ZnAcMP8. In addition, the solvent deuterium isotope effect ( $k_{\text{H}_2\text{O}}/k_{\text{D}_2\text{O}}$ ) is smaller in the protein, reflecting greater cofactor protection. The folded protein has the longest triplet lifetime of  $\sim 10$  ms and smallest isotope effect of 1.2, as expected for the least exposed Zn-porphyrin. The cofactor in the denatured protein appears to be only partially exposed; although triplet decay is faster than in the folded protein, it is still slower than in ZnAcMP8.

### 2.3.3 Isotope Effect in Singlet Excited States

Ideally, protein folding experiments would provide information at each step in the folding process, rather than an overall average. In order to take snapshots of hydration during folding, the measured lifetime needs to be shorter than the time it takes the protein to fold. Since the triplet state lifetime of folded Zn-cyt *c* is  $\sim 10$  ms, its folding reaction must be considerably longer. It was hoped the much shorter lived singlet state of Zn-porphyrins would exhibit similar isotope effects to the triplet state, therefore allowing time points along the reaction pathway to be sampled. The singlet excited state is deactivated mainly through intersystem crossing to the triplet state and fluorescence back to the ground state, leaving a small percentage of the singlet state population to decay through other radiationless events, such as coupling to the solvent. One main difference between the singlet excited state and the triplet excited state is their energetics of emission: the energy of the  $S_1 \rightarrow S_0$  transition is  $16806 \text{ cm}^{-1}$  while the  $T_1 \rightarrow S_0$  transition is  $13698 \text{ cm}^{-1}$ .<sup>9</sup> As no consistent isotope effect was observed in the singlet states of either ZnAcMP8 or Zn-cyt *c* under any conditions, most likely the higher energy gap of the singlet state reduces the probability of observing a difference in coupling to the solvent between  $\text{H}_2\text{O}$  and  $\text{D}_2\text{O}$ . Unfortunately, it seems the singlet excited state provides no



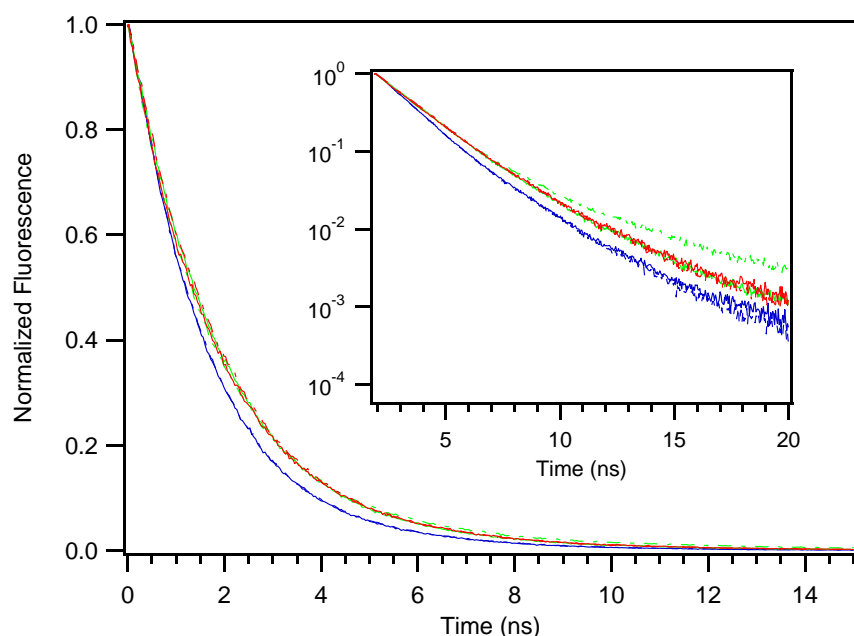


**Figure 2.6.** Fluorescence decays of Zn-cyt *c* singlet excited state in H<sub>2</sub>O (solid) and D<sub>2</sub>O (dashed) solutions, pH = pD = 7.4. Buffers were 20 mM phosphate (blue) with ~5 M GdmCl (green) or ~9 M urea (red).

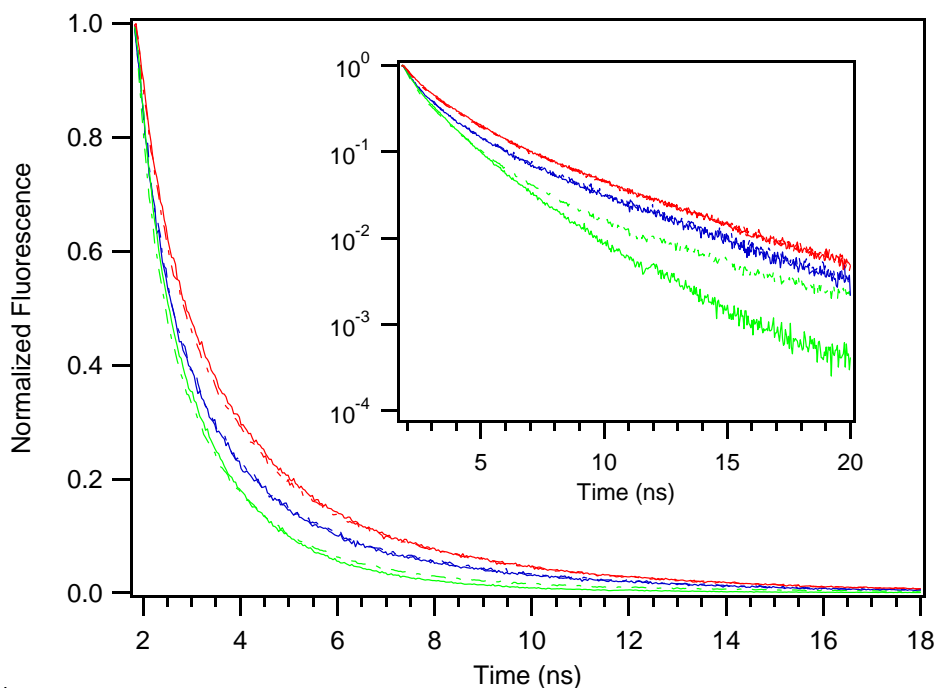


**Figure 2.7.** Fluorescence decays of Zn-AcMP8 singlet excited state in H<sub>2</sub>O (solid) and D<sub>2</sub>O (dashed) solutions; 0.1% TFA was added to the buffer. Buffers were 20 mM phosphate (blue) with ~5 M GdmCl (green) or ~9 M urea (red).

information on the exposure of the porphyrin to the solvent.

### 2.3.4 Bimolecular Quenching Experiments

The degree of solvent exposure of the Zn-porphyrin was further explored in a series of bimolecular quenching experiments with  $\text{Ru}(\text{NH}_3)_6^{3+}$ . Figures 2.8 (A) and (C) display decay traces of folded and unfolded triplet Zn-cyt *c* in the presence of quencher. When  $[\text{Ru}^{3+}] = 0.8 \text{ mM}$ , the majority decay component in the folded state is  $7630 \text{ s}^{-1}$ , which is 76 times faster than the triplet decay rate of  $\sim 100 \text{ s}^{-1}$  in the absence of quencher (a rate similar to one obtained in a previous study).<sup>23</sup> For the fully unfolded protein, triplet decays increase 500-800 times upon addition of quencher from pure decay rates of 810 (GdmCl) and 720 (urea)  $\text{s}^{-1}$  to  $4.4\text{--}6.4 \times 10^5$  and  $4.8 \times 10^5 \text{ s}^{-1}$ , respectively. This increase in quenching rate is primarily due to greater porphyrin accessibility to the quencher in the unfolded protein, and may also reflect the change in ionic strength in the GdmCl case.<sup>25,26</sup> Partially unfolded protein was monitored near the GdmCl and urea midpoints of 2.9 and 6.9 M, respectively. Near denaturant midpoints, the lifetimes are biexponential, with slow (40-70%) and fast (60-30%) components corresponding to compact and extended structures. The second-order rate constants are  $6.6 \times 10^8$  (extended) and  $5.9 \times 10^7$  (compact)  $\text{M}^{-1} \text{ s}^{-1}$  in GdmCl, and  $6.3 \times 10^8$  (extended) and  $8.6 \times 10^6$  (compact)  $\text{M}^{-1} \text{ s}^{-1}$  in urea. These rate constants are similar to those obtained in our previous work.<sup>17</sup> Figures 2.8 (B) and (D) illustrate the increase in triplet decay rates upon continual addition of quencher from 0.1 to  $\sim 5 \text{ mM}$ .

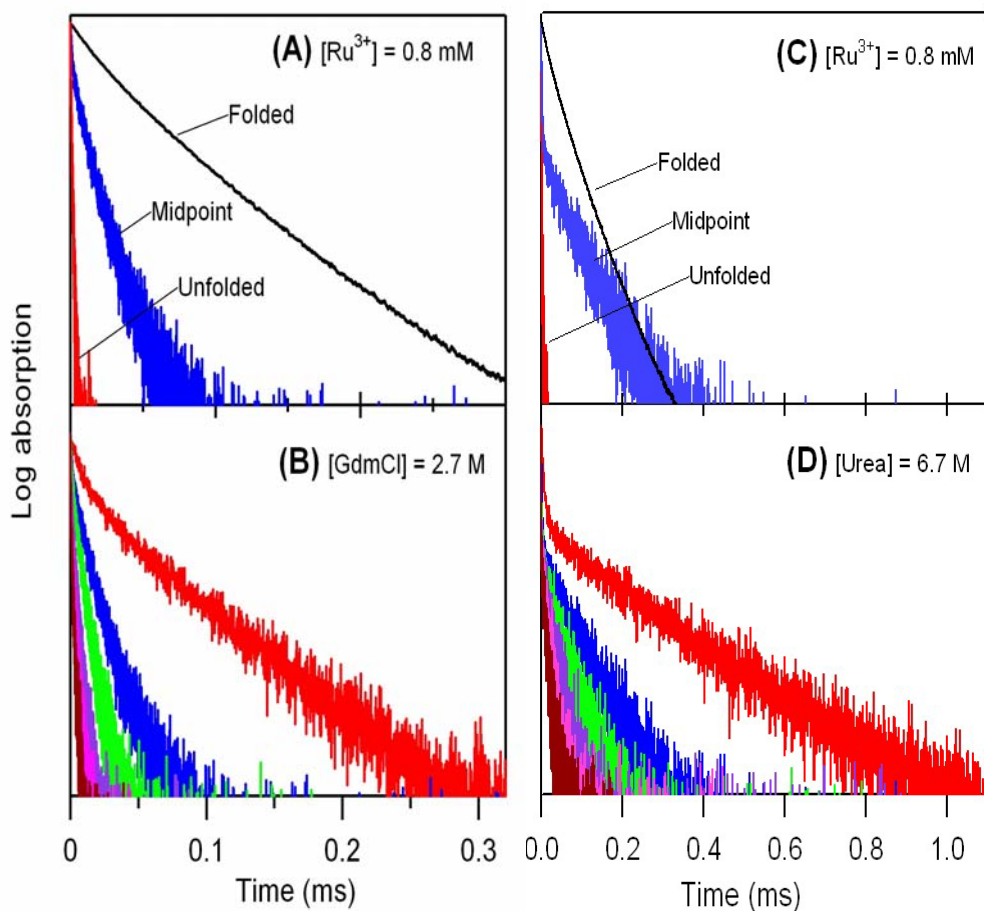


**Figure 2.8.** Transient absorption decay kinetics of triplet Zn-cyt *c* in 20 mM phosphate + GdmCl (left) and urea (right) solutions. (A) [GdmCl] = 0 M (black), 2.7 M (blue), and 5.6 M (red) with [Ru<sup>3+</sup>]=0.8 mM; (B) [Ru<sup>3+</sup>] = 0.3 (red), 0.8 (blue), 1.3 (green), 2.4 (purple), 3.3 (pink) and 4.5 (maroon) mM with [GdmCl] = 2.7 M; (C) [Urea] = 0 M (black), 6.7 M (blue), and 8.6 M (red) with [Ru<sup>3+</sup>] = 0.8 mM; and (D) [Ru<sup>3+</sup>] = 0.3 (red), 0.8 (blue), 1.4 (green), 2.4 (purple), 3.7 (pink) and 4.9 (maroon) mM with [urea] = 6.7 M. Note different timescales.

## 2.4 CONCLUSIONS

### 2.4.2 Zn-porphyrin solvation in Folded Zn-cyt *c*

The cofactor in folded Zn-cyt *c* is partially hydrated, as indicated by the modest, yet reproducible, isotope effect  $k_{\text{H}_2\text{O}}/k_{\text{D}_2\text{O}}$  of 1.2 (Table 2.1 and Figure 2.5). This isotope effect is smaller than that observed for the fully exposed Zn-porphyrin in ZnAcMP8 ( $k_{\text{H}_2\text{O}}/k_{\text{D}_2\text{O}} \sim 1.5$ ), and the triplet lifetime of the folded protein ( $\tau \sim 10$  ms) is much longer than that for ZnAcMP8 ( $\tau \sim 0.3$  ms). The difference in lifetimes arises because the folded protein restricts solvent access to the cofactor. The observed isotope effect of 1.2 in buffer may be explained by the presence of water molecules in the Zn-porphyrin binding pocket of the folded protein combined with partial cofactor exposure to the bulk solvent. Several internal water molecules are present in crystals of horse heart ferro- and ferricytochrome *c*, including two believed to interact with the heme.<sup>27</sup> One of these heme-associated water molecules moves  $\sim 4$  Å away from the metal upon oxidation of Fe(II) to Fe(III),<sup>28</sup> suggesting that buried structural waters in cytochrome *c* play a role in solvent reorganization associated with electron transfer.<sup>29</sup> The observation that numerous H<sub>2</sub>O molecules occupy conserved positions in a variety of cytochromes *c* indicates that these solvent molecules are critical for protein function.<sup>27</sup>

The internal water molecules in folded cytochrome *c* and other proteins are dynamic and exchangeable, as supported by experimental and theoretical studies of water penetration, mobility, and exchange in folded proteins.<sup>30-35</sup> A great deal of NMR work has revealed that surface-bound waters exchange rapidly (pico- to nanoseconds), while buried solvent molecules have much longer residence times (micro- to milliseconds).<sup>32-35</sup> In contrast to these ordered molecules, crystallographically invisible, disordered solvent

molecules may reside in highly hydrophobic cavities for up to hundreds of microseconds.<sup>34</sup> Based on our observation of an isotope-sensitive triplet state in Zn-cyt *c*, we suggest that at least some of the water molecules in the cofactor binding pocket are rapidly mobile.

### 2.4.3 Bimolecular Quenching

In addition to these internal waters, the porphyrin is hydrated in part by the bulk solvent, as indicated by several lines of evidence. First, our observation of triplet state quenching by Ru(NH<sub>3</sub>)<sub>6</sub><sup>3+</sup> in the folded protein (Figure 2.8 A)<sup>3</sup> confirms that the porphyrin is accessible to bulk solvent. Second, the X-ray crystal structure reveals that ~8% of the heme group in Fe(III)-cyt *c* is exposed to solvent, and this exposed region is encircled by charged residues.<sup>27</sup> Finally, under folding conditions, metal-free cytochrome *c* has exchangeable pyrrolic protons,<sup>18,34</sup> as evidenced by a relatively large isotope effect ( $k_{\text{H}_2\text{O}}/k_{\text{D}_2\text{O}} = 2.2$ ) associated with triplet decay.<sup>18</sup> This large isotope effect arises because changes in intramolecular vibrations upon deuteration of the metal-free porphyrin affect the strength of coupling between the triplet and ground states. The upper limit for an isotope effect arising primarily from solvent coupling is 1.5, and this value of  $k_{\text{H}_2\text{O}}/k_{\text{D}_2\text{O}}$  is similar to that observed for relatively small organometallic molecules in protic solvents.<sup>20</sup> While the relatively long lifetime of the Zn-porphyrin triplet state reported here and elsewhere<sup>18,23,25</sup> is consistent with a buried cofactor in the folded protein, other results and observations (e.g., proton exchange, an isotope effect of 1.2, and partial cofactor exposure in the crystal structure) confirm that at least a some of the porphyrin must be exposed to solvent.

#### **2.4.4 Summary**

We have demonstrated that Zn-porphyrin triplet lifetimes are sensitive indicators of heme-pocket hydration. Our finding that folded and unfolded species have different isotope effects and bimolecular quenching rates indicates that changes in hydration can be monitored during a folding reaction. Important issues such as the timescales for water expulsion,<sup>35</sup> the nature of dehydrated and hydrated intermediates, and even the effect of denaturant on folding pathways can be addressed by means of triplet lifetime measurements.

## **2.7 MATERIALS AND METHODS**

### **2.7.2 Preparation of ZnAcMP8, Zn-cyt *c* and Zn-cyt *c*'**

*The work to produce AcMP8 was completed by Dr. Judy E. Kim.*

AcMP8 was prepared from horse heart cytochrome *c* (Sigma) following a literature procedure.<sup>36</sup> Lyophilized AcMP8 was treated with anhydrous HF at -78 °C to create metal-free AcMP8 (Beckman Institute Biopolymer Synthesis Facility) which, when dissolved in 100 mM potassium acetate buffer (pH 5.0), displayed a broad Soret absorption at 391 nm and smaller bands at 506, 540, 568 and 620 nm, characteristic of free base porphyrins. Subsequent steps were performed in the dark. Zinc acetate was added to a final concentration of 10 mM, and this solution was stirred in a 55 °C water bath for 2 h. Zinc incorporation was confirmed by a shift in the Soret absorption from 391 nm to a sharp peak at 406 nm. Crude ZnAcMP8 was washed and the buffer was exchanged to a 6% acetonitrile, 0.1% TFA solution using ultrafiltration. Pure ZnAcMP8 was obtained after purification on a reverse phase column (Pep-RPC 16/10, Amersham

Biosciences) using a linear gradient up to 60% acetonitrile. ZnAcMP8 was then washed, concentrated, and stored in aqueous 6% acetonitrile, 0.1% TFA solution at -80 °C.

Zn-cyt *c* was prepared using a modified literature procedure.<sup>37</sup> Horse heart cytochrome *c* (Sigma) was treated with anhydrous HF at -78 °C to remove the iron center. Subsequent steps were performed in the dark. The metal free protein was dissolved in 100 mM potassium acetate buffer (pH 5.0) and heated to 55 °C at which point 10 mM zinc acetate was added. After approximately 30 minutes, the zinc incorporation was confirmed by a shift in absorbance from 404 nm to 423 nm. The excess zinc and salts were removed via dialysis into 20 mM potassium phosphate buffer (pH 7.0) and the protein was further purified by FPLC (HiTrap CM cation exchange column, Amersham Biosciences) and eluted with a linear gradient to 0.5 M NaCl. Samples with an  $A_{423}/A_{549}$  value higher than 15.8 were concentrated and stored at -80 °C.

### **2.7.3 Preparation of Deuterated Buffers**

Urea- $d_4$  (Sigma) was recrystallized from D<sub>2</sub>O (99.9%, Cambridge Isotope Laboratories). Guanidine- $d_5$  deuteriochloride was made by dissolving guanidine hydrochloride (Sigma) in D<sub>2</sub>O (99.9%, Cambridge Isotope Laboratories), followed by repeated recrystallization or solvent evaporation. Isotopic purity was determined by Raman spectroscopy using 514 nm excitation and a spectrograph-CCD detector system. Both protonated and deuterated denaturants had > 95% purity.

### **2.7.4 Sample Preparation**

The 1-4  $\mu$ M Zn-cyt *c* (20 mM phosphate, pH=pD=7.4) and ZnAcMP8 (2-3  $\mu$ M in 20 mM phosphate + 0.1% TFA) solution was transferred to a 1-cm quartz cuvette with a 14/20 frosted glass joint. A rubber septum sealed in the solution and a small stirbar.

Using a syringe attached to a schlenk line, complete with a Oxiclear oxygen scrubber, the headgas of the cuvette was evacuated and refilled with argon gas. After this quick pump/purge cycle was repeated twice, the syringe was then submerged in the protein solution. The addition of an outlet needle in the septum allowed the argon gas to be bubbled through the protein solution. Typically, thirty minute of sparging were required to eliminate the oxygen from the system, after which the protein is much less light sensitive. The bimolecular quencher was syringed into each sample prior to the sparging step. Denaturant concentrations were determined after each experiment by index of refraction measurements.

### 2.7.5 Transient Absorption Experiments

Transient absorption spectra of the Zn-porphyrin triplet in ZnAcMP8 and Zn-cyt *c* were measured; the change in absorbance from 420-500 nm due to formation of triplet state in ZnAcMP8 is displayed in Figure 2.1 along with the ground-state absorption spectrum. The triplet ZnAcMP8 exhibits an absorption maximum near 440 nm, whereas triplet Zn-cyt *c* absorbs strongly near 460 nm, consistent with previous results.<sup>34,39</sup> Comparison with the ground-state Zn-cyt *c* bleach reveals an increase in molar extinction coefficient of 30-40 mM<sup>-1</sup> cm<sup>-1</sup> at 450 nm upon formation of triplet Zn-cyt *c*. Thus, 450 nm is an excellent probe wavelength for the Zn-porphyrin triplet state, since ground-state absorption, cation radical absorption ( $\lambda_{\max} \sim 675$  nm),<sup>23</sup> and triplet luminescence ( $\lambda_{\max} \sim 736$  nm) are minimal at this wavelength.<sup>23,38</sup> A 10 Hz, 10 ns Nd:YAG laser with a 355 nm-pumped optical parametric oscillator was used to form the transient triplet state of Zn-porphyrin. The probe was a continuous-wave 75 W xenon arclamp. The 550 nm, 1.6-mm diameter pump and 450 nm, 0.7-mm diameter probe beams were collinear in a 1-cm



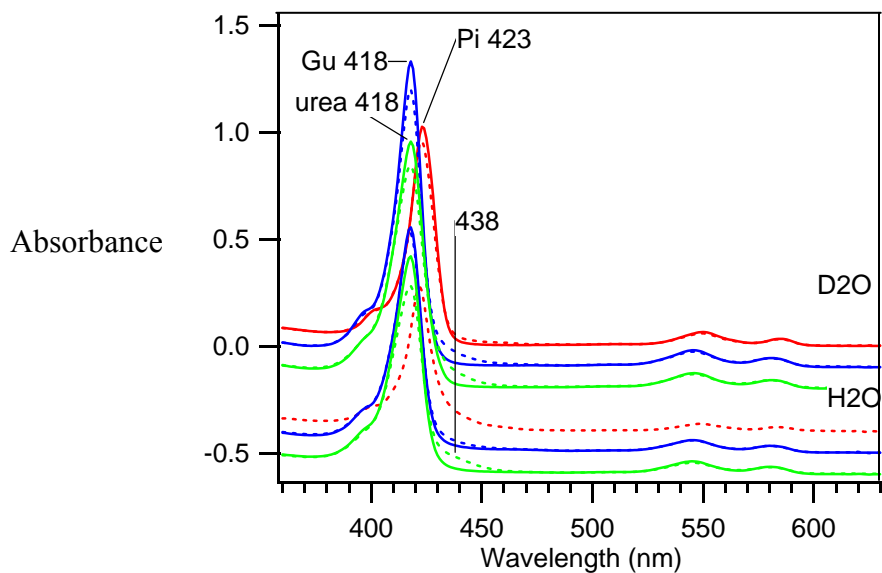


**Figure 2.9.** UV-Vis spectra of Zn-cyt *c* in 20 mM phosphate (red), GdmCl (blue) and urea (green) solutions, before (solid) and after (dashed) laser excitation. The  $\lambda_{\text{max}}$  of the Soret in each condition is indicated; H<sub>2</sub>O and D<sub>2</sub>O are indicated as well.

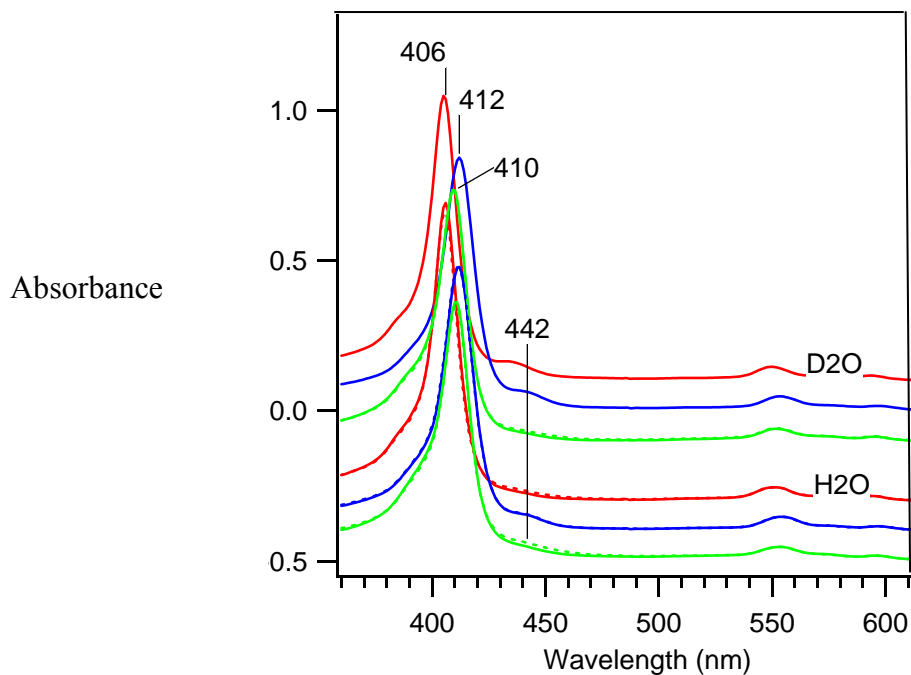


**Figure 2.10.** UV-Vis spectra of Zn-AcMP8 in 20 mM phosphate (red), GdmCl (blue) and urea (green) solutions with 0.1% TFA, before (solid) and after (dashed) laser excitation. The  $\lambda_{\text{max}}$  of the Soret in each condition is indicated; H<sub>2</sub>O and D<sub>2</sub>O are indicated as well.

quartz cuvette. Signal light was dispersed in a 10-cm, F/3.5 double monochromator (DH10, Instruments, S.A.) and detected by a PMT. Power dependence experiments verified that under these conditions, pump (1.0-1.5 mW) and probe (1.8-2.3 mW) powers were well within the linear regime for triplet formation and decay. Reported kinetics curves are the average of 1000 shots, and photodegradation of the degassed 1-4  $\mu\text{M}$  Zn-cyt *c* solutions (20 mM phosphate, pH=pD=7.4) monitored by UV/vis absorption spectroscopy was typically <10% after each experiment (Figure 2.9). For ZnAcMP8 (2-3  $\mu\text{M}$  in 20 mM phosphate + 0.1% TFA) bimolecular quenching experiments with  $\text{Ru}(\text{NH}_3)_6^{3+}$ , no photodegradation was detected (Figure 2.10). A prior study<sup>18</sup> did not resolve the modest isotope effect we have found for triplet Zn-cyt *c*, presumably due to less sensitive detection.

### **2.7.6 Singlet Excited States of Zn-Cyt *c* and Zn-MP8**

The second harmonic of a regeneratively amplified femtosecond Ti:sapphire laser (SpectraPhysics) was used to excite the singlet state of Zn-cyt *c* and ZnAcMP8 at 435 nm. The detector was a picosecond streak camera (Hamamatsu C5680, Ichinocho, Japan). The streak camera was used in the photon-counting mode (5000 counts per sample) for luminescence-decay measurements ranging from 5 ns to 20 ns. Although oxygen quenching is not on the timescale of these experiments, the samples were quickly pump/purged as a precaution.

## REFERENCES

- (1) Papoian, G. A.; Ulander, J.; Eastwood, M. P.; Luthey-Schulten, Z.; Wolynes, P. G. Water in Protein Structure Prediction. *Proc. Natl. Acad. Sci. USA* **2004**, *101*, 3352-3357.
- (2) Papoian, G. A.; Ulander, J.; Wolynes, P. G. Role of Water Mediated Interactions in Protein-protein Recognition Landscapes. *J. Am. Chem. Soc.* **2003**, *125*, 9170-9178.
- (3) Cheung, M. S.; Garcia, A. E.; Onuchic, J. N. Protein folding mediated by solvation: Water expulsion and formation of the hydrophobic core occur after the structural collapse. *Proc. Natl. Acad. Sci. USA* **2002**, *99*, 685-690.
- (4) Sheinerman, F. B.; Brooks III, C. L. Calculations on folding of segment B1 of streptococcal protein G. *J. Mol. Biol.* **1998**, *278*, 439-456.
- (5) Fernandez-Escamilla, A. M.; Cheung, M. S.; Vega, M. C.; Wilmanns, M.; Onuchic, J. N.; Serrano, L. Solvation in protein folding analysis: Combination of theoretical and experimental approaches. *Proc. Natl. Acad. Sci. USA* **2004**, *101*, 2834-2839.
- (6) Sorenson, J. M.; Hura, G.; Soper, A. K.; Pertsemlidis, A.; Head-Gordon, T. Determining the role of hydration forces in protein folding. *J. Phys. Chem. B* **1999**, *103*, 5413-5426.
- (7) Finkelstein, A.V.; Shakhnovich, E.I. Theory of Cooperative Transitions in Protein Molecules. *Biopolymers* **1989**, *28*, 1681-1694.
- (8) Garcia, A. E.; Hummer, G. Water Penetration and Escape in Proteins. *Proteins* **2000**, *38*, 261-272.
- (9) Dunbar, J.; Yennawar, H. P.; Banerjee, S.; Luo, J.; Farber, G. K. The Effect of Denaturants on Protein Structure. *Protein Science* **1997**, *6*, 1727-1733.
- (10) Vanzi, F.; Madan, B.; Sharp, K. Effect of the Protein Denaturants Urea and Guanidinium on Water Structure: A Structural and Thermodynamic Study. *J. Am. Chem. Soc.* **1998**, *120*, 10748-10753.
- (11) Shastry, M. C. R.; Sauder, J. M.; Roder, H. Kinetic and Structural Analysis of Submillisecond Folding Events in Cytochrome *c*. *Acc. Chem. Res.* **1998**, *31*, 717-725.
- (12) Englander, S. W.; Sosnick, T. R.; Mayne, L. C.; Shtilerman, M.; Qi, P. X.; Bai, Y. Fast and Slow Folding in Cytochrome *c*. *Acc. Chem. Res.* **1998**, *31*, 737-744.
- (13) Winkler, J. R. Cytochrome *c* Folding Dynamics. *Curr. Opin. Chem. Bio.* **2004**, *8*, 169-174.

- (14) Anni, H.; Vanderkooi, J. M.; Mayne, L. C. Structure of Zinc-substituted Cytochrome *c*-Nuclear Magnetic Resonance and Optical Spectroscopic Studies. *Biochemistry* **1995**, *34*, 5744-5753.
- (15) Banci, L.; Bertini, I.; Huber, J. G.; Spyroulias, G. A.; Turano, P. Solution Structure of Reduced Horse Heart Cytochrome *c*. *J. Biol. Inorg. Chem.* **1999**, *4*, 21-31.
- (16) Mines, G. A.; Winkler, J. R.; Gray, H. B. Spectroscopic Studies of Ferrocycytochrome *c* Folding. In *Spectroscopic Methods in Bioinorganic Chemistry*; Solomon, E.; Hodgson, K., eds. American Chemical Society: Washington, D.C., 1997; Vol. 692, pp 188-211.
- (17) Lee, J. C.; Chang, I.; Gray, H. B.; Winkler, J. R. The Cytochrome *c* Folding Landscape Revealed by Electron-transfer Kinetics. *J. Mol. Biol.* **2002**, *320*, 159-164.
- (18) Sudha, B. P.; Dixit, S. N.; Moy, V. T.; Vanderkooi, J. M. Reaction of Excited-state Cytochrome *c* Derivatives- Delayed Fluorescence and Phosphorescence of Zinc, Tin, and Metal-free Cytochrome *c* at Room Temperature. *Biochemistry* **1984**, *23*, 2103-2107.
- (19) Caspar, J. V.; Sullivan, B. P.; Kober, E. M.; Meyer, T. J. Application of the Energy-gap Law to the Decay of Charge-transfer Excited States-Solvent Effects. *Chem. Phys. Lett.* **1982**, *91*, 91-95.
- (20) Caspar, J. V.; Meyer, T. J. Photochemistry of Ru(Bpy)<sub>3</sub><sup>2+</sup>-Solvent Effects. *J. Am. Chem. Soc.* **1983**, *105*, 5583-5590.
- (21) Meyer, T. J. Photochemistry of Metal Coordination Complexes-Metal to Ligand Charge-Transfer Excited-States. *Pure and Appl. Chem.* **1986**, *58*, 1193-1206.
- (22) Lyubovitsky, J.G.; Gray, H.B.; Winkler, J.R. Mapping the Cytochrome *c* Folding Landscape. *J. Am. Chem. Soc.* **2002**, *124*, 5481-5485.
- (23) Elias, H.; Chou, M. H.; Winkler, J. R. Electron-Transfer Kinetics of Zn-substituted Cytochrome *c* and Its Ru(NH<sub>3</sub>)<sub>5</sub>(Histidine-33) Derivative. *J. Am. Chem. Soc.* **1988**, *110*, 429-434.
- (24) Low, D. W.; Gray, H. B.; Duus, J. O. Paramagnetic NMR Spectroscopy of Microperoxidase-8. *J. Am. Chem. Soc.* **1997**, *119*, 1-5.
- (25) Tremain, S. M.; Kostic, N. M. Molten-globule and Other Conformational Forms of Zinc Cytochrome *c*. Effect of Partial and Complete Unfolding of the Protein on its Electron-transfer Reactivity. *Inorg. Chem.* **2002**, *41*, 3291-3301.

- (26) Wherland, S.; Gray, H. B. Metalloprotein Electron-transfer Reactions- Analysis of Reactivity of Horse Heart Cytochrome *c* with Inorganic Complexes. *Proc. Natl. Acad. Sci. USA* **1976**, *73*, 2950-2954.
- (27) Bushnell, G. W.; Louis, G. V.; Brayer, G. D. High-resolution 3-dimensional Structure of Horse Heart Cytochrome *c*. *J. Mol. Biol.* **1990**, *214*, 585-595.
- (28) Qi, P. X.; Urbauer, J. L.; Fuentes, E. J.; Leopold, M. F.; Wand, A. J. Structural Water in Oxidized and Reduced Horse Heart Cytochrome *c*. *Nat. Struct. Biol.* **1994**, *1*, 378-382.
- (29) Muegge, I.; Qi, P. X.; Wand, A. J.; Chu, Z. T.; Warshel, A. The Reorganization Energy of Cytochrome *c* Revisited. *J. Phys. Chem. B* **1997**, *101*, 825-836.
- (30) Makarov, V.; Pettitt, B. M.; Feig, M. Solvation and Hydration of Proteins and Nucleic Acids: A Theoretical View of Simulation and Experiment. *Acc. Chem. Res.* **2002**, *35*, 376-384.
- (31) Phillips Jr., G. N.; Pettitt, B. M. Structure and Dynamics of the Water Around Myoglobin. *Protein Science* **1995**, *4*, 149-158.
- (32) Gottschalk, M.; Dencher, N. A.; Halle, B. Microsecond Exchange of Internal Water Molecules in Bacteriorhodopsin. *J. Mol. Biol.* **2001**, *311*, 605-621.
- (33) Otting, G.; Liepinsh, E.; Wuthrich, K. Protein Hydration in Aqueous Solution. *Science* **1991**, *254*, 974-980.
- (34) Ernst, J. A.; Clubb, R. T.; Zhou, H.-X.; Gronenborn, A. M.; Clore, G. M. Demonstration of Positively Disordered Water Within a Protein Hydrophobic Cavity by NMR. *Science* **1995**, *267*, 1813-1817.
- (35) Denisov, V. P.; Halle, B. Hydration of Denatured and Molten Globule Proteins. *Faraday Discuss.* **1996**, *103*, 227-244.
- (40) Li, R.; Woodward, C. The Hydrogen Exchange Core and Protein Folding. *Protein Science* **1999**, *8*, 1571-1591.
- (41) Zentko, S.; Scarrow, R. C.; Wright, W. W.; Vanderkooi, J. M. Protonation of Porphyrin in Iron-free Cytochrome *c*: Spectral Properties of Monocation Free Base Porphyrin, a Charge Analogue of Ferric Heme. *Biospectroscopy* **1999**, *5*, 141-150.
- (42) Low, D. W.; Winkler, J. R.; Gray, H. B. Photoinduced Oxidation of Microperoxidase-8: Generation of Ferryl and Cation-radical Porphyrins. *J. Am. Chem. Soc.* **1996**, *118*, 117-120.

- (43) Ye, S.; Shen, C.; Cotton, T. M.; Kostic, N. M. Characterization of Zinc-substituted Cytochrome c by Circular Dichroism and Resonance Raman Spectroscopic Methods. *J. Inorg. Biochemistry* **1997**, *65*, 219-226.
- (44) Vanderkooi, J. M.; Adar, F.; Erecinska, M. Metallocytochromes c-Characterization of Electronic Absorption and Emission Spectra of Sn<sup>4+</sup> and Zn<sup>2+</sup> Cytochromes c. *Eur. J. Biochemistry* **1976**, *64*, 381-387.